J. Fluid Mech. (1982), *vol.* 120, *pp.* 267–281
Printed in Great Britain

Nonlinear-wave effects on fixed and floating bodies

By MICHAEL DE St Q. ISAACSON

Department of Civil Engineering, University of British Columbia,
Vancouver, B.C., Canada

A numerical method for calculating the interaction of steep (nonlinear) ocean waves with large fixed or floating structures of arbitrary shape is described. The interaction is treated as a transient problem with known initial conditions corresponding to still water in the vicinity of the structure and a prescribed incident waveform approaching it. The development of the flow, together with the associated fluid forces and structural motions, are obtained by a time-stepping procedure in which the flow at each time step is calculated by an integral-equation method based on Green's theorem. A few results are presented for two reference situations and these serve to illustrate the effects of nonlinearities in the incident waves.

1. Introduction

Wave-force predictions for large fixed or floating offshore structures are generally made on the basis of linear diffraction theory, which is formally valid for small-amplitude sinusoidal waves (for a review of the methods used see Sarpkaya & Isaacson 1981). In order to account more realistically for the effect of large wave heights, research has recently been directed primarily towards developing a second approximation based on the Stokes expansion procedure. However, such an approach is of practical value only under somewhat restricted conditions, as in the case of an undisturbed wavetrain described by Stokes' second-order theory. On the other hand, considerable progress has now also been made on the accurate calculation of two-dimensional (vertical-plane) flows describing the deformation of steep or breaking waves (Longuet-Higgins & Cokelet 1976; Srokosz 1981), even when a fixed obstacle is present in the flow (Vinje & Brevig 1981). The methods used rely on the assumption that the corresponding flows are two-dimensional, and cannot be directly extended to three-dimensional problems.

Using a different approach from the two above, an attempt is made in the present paper to provide a numerical solution to the complete boundary-value problem in three dimensions and without applying any wave-height perturbation procedure. The method described here is applicable to the general case of a body of arbitrary shape which may also undergo free or restrained motions. In the approach adopted, the wave diffraction is treated as a transient problem with known initial conditions corresponding to still water in the vicinity of the structure and a prescribed incident waveform approaching the structure. The development of the flow can then be obtained by a time-stepping procedure, in which the velocity potential of the flow at any one instant is obtained by an integral-equation method based on Green's theorem. Simplifications to the method corresponding to the two-dimensional vertical-plane

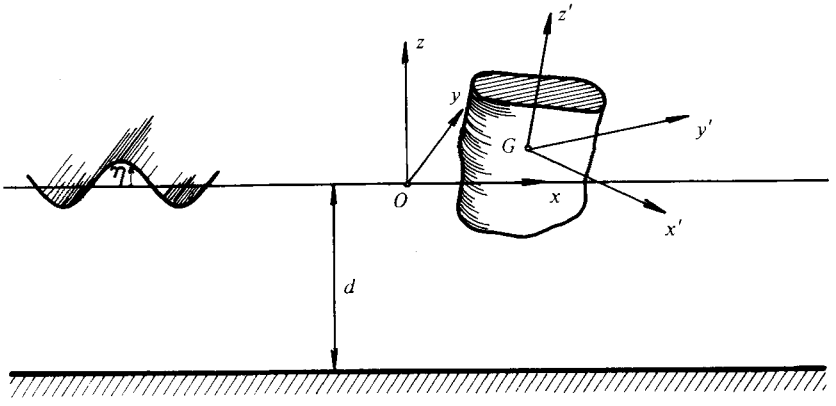

FIGURE 1. Definition sketch.

problem, or to the cases of a structure which is fixed or undergoing forced motions are also described. A preliminary formulation of the method, which dealt with the fixed-body case only, has been described in detail in an unpublished report (Isaacson 1981*a*), and subsequently summarized (Isaacson 1981*b*).

2. Theoretical formulation

Since the body motions are not linearized in the usual way, it is convenient to employ two co-ordinate systems as indicated in figure 1. *Oxyz* forms a right-handed Cartesian co-ordinate system fixed in space, with x measured in the direction of incident wave propagation and z measured upwards from the still-water level. G is the centre of mass of the body and $Gx'y'z'$ forms a right-handed Cartesian co-ordinate system fixed to the body such that the axes coincide with the body's principal axes of inertia. In most cases, we may take x' to form the longitudinal axis, y' the transverse axis, and the z' axis is initially directed upwards.

At any instant the location of the body is completely specified by the co-ordinates $\zeta_1, \zeta_2, \ldots, \zeta_6$, where $(\zeta_1, \zeta_2, \zeta_3)$ denote the co-ordinates of G in the $Oxyz$ system and so describe the translation of the body; and $(\zeta_4, \zeta_5, \zeta_6)$ denote the angles of roll, pitch and yaw measured clockwise when facing the positive x', y' and z' directions in turn (for their formal definitions see Landweber 1961).

In the following development (based on Landweber 1961) it is more convenient to express the body motions in terms of $u_1, u_2, \ldots, u_6$, where u_1, u_2 and u_3 are the components of the absolute velocity of G in the x', y' and z' directions respectively; and u_4, u_5 and u_6 are the angular-velocity components of the body about the x', y' and z' axes respectively. ζ_k and u_k are related as follows:

$$\left.\begin{aligned} \dot{\zeta}_4 - \dot{\zeta}_6 s_5 &= u_4, \\ \dot{\zeta}_6 s_4 c_5 + \dot{\zeta}_5 c_4 &= u_5, \\ \dot{\zeta}_6 c_4 c_5 - \dot{\zeta}_5 s_4 &= u_6; \end{aligned}\right\} \tag{2.1}$$

$$\left.\begin{aligned} \dot{\zeta}_1 &= u_1 c_5 c_6 + u_2(s_4 s_5 s_6 - c_4 s_6) + u_3(c_4 s_5 c_6 + s_4 s_6), \\ \dot{\zeta}_2 &= u_1 c_5 s_6 + u_2(s_4 s_5 s_6 + c_4 c_6) + u_3(c_4 s_5 s_6 - s_4 c_6), \\ \dot{\zeta}_3 &= -u_1 s_5 + u_2 s_4 c_5 + u_3 c_4 c_5; \end{aligned}\right\} \tag{2.2}$$

where dots denote differentiation with respect to time, and c_k and s_k denote $\cos\zeta_k$ and $\sin\zeta_k$ respectively.

The boundary-value problem defining the fluid motion may be set up as follows. Let t denote time and η the free-surface elevation above the still-water level. The sea bed is assumed horizontal along the plane $z = -d$. The fluid is assumed incompressible and inviscid, and the flow irrotational. The fluid motion can therefore be described by a velocity potential ϕ, which satisfies the Laplace equation within the fluid region,

$$\nabla^2\phi = 0, \tag{2.3}$$

and is subject to the following boundary conditions:

$$\frac{\partial\phi}{\partial z} = 0 \quad \text{at} \quad z = -d, \tag{2.4}$$

$$\frac{\partial\phi}{\partial n} = V_n \quad \text{on } S_\mathrm{b}, \tag{2.5}$$

$$\frac{\partial\phi}{\partial n} - \dot{\eta}n_z = 0 \quad \text{on } S_\mathrm{f}, \tag{2.6}$$

$$\dot{\phi} + g\eta + \tfrac{1}{2}(\nabla\phi)^2 = 0 \quad \text{on } S_\mathrm{f}. \tag{2.7}$$

Here g is the acceleration due to gravity, n denotes distance in the direction of the unit normal vector $\mathbf{n}$ directed outward from the fluid region, V_n is the velocity of the body surface in the direction $\mathbf{n}$, S_b is the immersed body surface, S_f is the free surface ($z = \eta$), and n_z is the direction cosine of $\mathbf{n}$ with respect to the z-direction. Equations (2.4) and (2.5) correspond to the kinematic boundary conditions on the sea bed and body surface respectively, while (2.6) and (2.7) correspond to the kinematic and dynamic free-surface boundary conditions respectively. (The form of (2.6) adopted here is accounted for in Isaacson 1981*a*.)

V_n at the point $\mathbf{x} = (x', y', z')$ on the body surface may be expressed in terms of u_k by

$$V_n = \sum_{k=1}^{6} n_k u_k, \tag{2.8}$$

where

$$\left.\begin{aligned} &n_1 = n_{x'}, \quad n_2 = n_{y'}, \quad n_3 = n_{z'}, \\ &n_4 = n_{z'}y' - n_{y'}z', \\ &n_5 = n_{x'}z' - n_{z'}x', \\ &n_6 = n_{y'}x' - n_{x'}y', \end{aligned}\right\} \tag{2.9}$$

and $n_{x'}$, $n_{y'}$, $n_{z'}$ are the direction cosines of $\mathbf{n}$ at $\mathbf{x}$ in the x', y', and z' directions respectively.

A boundary-integral method involving a Green function is used as the basis for a numerical evaluation of ϕ. Since ϕ is a harmonic function, the second form of Green's theorem may be applied over a closed surface S containing a fluid region, to relate boundary values of the potential ϕ and its normal derivative $\partial\phi/\partial n$ (see e.g. Kellogg 1929; Morse & Feshbach 1953). The potential $\phi(\mathbf{x})$ at the point $\mathbf{x}$ for the case where $\mathbf{x}$ lies on the boundary itself (approached from within the region contained by S) is expressed as

$$\phi(\mathbf{x}) = \frac{1}{2\pi}\int_S \left[G(\mathbf{x},\boldsymbol{\xi})\frac{\partial\phi}{\partial n}(\boldsymbol{\xi}) - \phi(\boldsymbol{\xi})\frac{\partial G}{\partial n}(\mathbf{x},\boldsymbol{\xi})\right] dS. \tag{2.10}$$

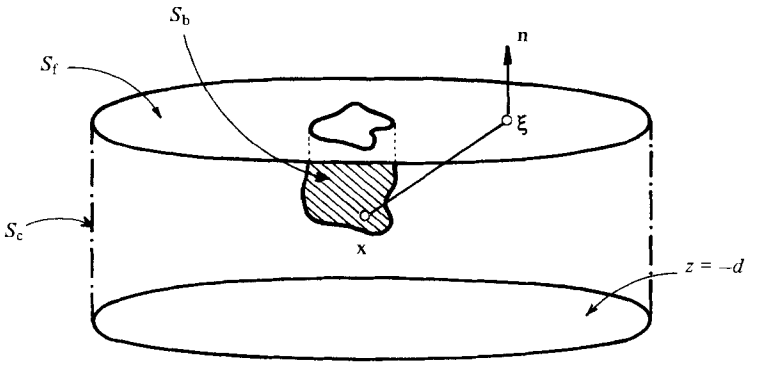

FIGURE 2. Sketch of integration surfaces (shown with $\eta = 0$).

Here $\boldsymbol{\xi}$ represents a point (ξ, η, ζ) on the surface S over which the integration is performed, G is a suitable Green function and n is measured from the point $\boldsymbol{\xi}$. (In (2.10) the surface S is assumed smooth at $\mathbf{x}$. Otherwise (2.10) may be modified by replacing the factor $1/2\pi$ by $1/\beta$, where β is the solid angle or the fluid side of $\mathbf{x}$ that S makes at $\mathbf{x}$.) In the present context the surface S would comprise the immersed body surface S_b, the instantaneous free surface S_f, a vertical control surface S_c surrounding the body and the sea bed, as indicated in figure 2. However, the assumption of a horizontal sea bed is generally quite reasonable, and it is more efficient to exclude the sea bed from S and to choose a Green function that accounts for the symmetry about the sea bed. This is

$$G = 1/r + 1/r', \tag{2.11}$$

where r is the distance between the points $\mathbf{x}$ and $\boldsymbol{\xi}$,

$$r = |\mathbf{x} - \boldsymbol{\xi}| = [(x-\xi)^2 + (y-\eta)^2 + (z-\zeta)^2]^{\frac{1}{2}}, \tag{2.12}$$

and r' is the distance between $\mathbf{x}$ and the point $\boldsymbol{\xi}' = (\xi, \eta, -(\zeta + 2d))$, which is the reflection of $\boldsymbol{\xi}$ in the sea bed,

$$r' = |\mathbf{x} - \boldsymbol{\xi}'| = [(x-\xi)^2 + (y-\eta)^2 + (z+\zeta+2d)^2]^{\frac{1}{2}}. \tag{2.13}$$

Initial conditions are chosen to correspond to still water in the vicinity of the structure and a known incident waveform approaching it. Any scattered waves subsequently generated by the interaction with the structure travel only a short distance over the duration that is analysed. Thus, provided that the control surface is chosen to lie sufficiently far from the body, the scattered waves will not reach it in this time. Consequently, the values of ϕ and $\partial\phi/\partial n$ on this surface correspond to those of the incident wave field, denoted by the superscript (w), which are known at all times from any chosen wave theory. That is

$$\left.\begin{aligned} \phi &= \phi^{(\mathrm{w})} \\ \frac{\partial \phi}{\partial n} &= \frac{\partial \phi^{(\mathrm{w})}}{\partial n} \end{aligned}\right\} \quad \text{on } S_c. \tag{2.14}$$

The location of the control surface that meets the above requirements can be estimated in terms of the time interval to be analysed and the speed of scattered-wave-energy propagation, which can be approximated by the group velocity calculated by

linear wave theory. It follows that the surface S_f should extend to about one or two wavelengths from the body surface, and so is not unduly large.

By applying (2.14) to (2.10) the surface integral is conveniently separated into an integral over S_c that is known at any time, and an integral over $S_b + S_f$ that contains the boundary functions ϕ and $\partial\phi/\partial n$ to be determined. That is

$$\phi(\mathbf{x}) = \frac{1}{2\pi}\int_{S_b+S_f}\left[G(\mathbf{x},\boldsymbol{\xi})\frac{\partial\phi}{\partial n}(\boldsymbol{\xi}) - \phi(\boldsymbol{\xi})\frac{\partial G}{\partial n}(\mathbf{x},\boldsymbol{\xi})\right]dS$$
$$+\frac{1}{2\pi}\int_{S_c}\left[G(\mathbf{x},\boldsymbol{\xi})\frac{\partial\phi^{(w)}}{\partial n}(\boldsymbol{\xi}) - \phi^{(w)}(\boldsymbol{\xi})\frac{\partial G}{\partial n}(\mathbf{x},\boldsymbol{\xi})\right]dS. \tag{2.15}$$

This integral equation over the surface $S_b + S_f$ is subject to boundary conditions on these two surfaces S_b and S_f.

The free-surface boundary conditions are treated by an explicit time-stepping procedure in which the free surface $S_{f(t+\Delta t)}$ and the velocity potential $\phi_{t+\Delta t}$ both at time $t+\Delta t$ are expressed explicitly in terms of the solution up to time t. Various time-differencing schemes may be used, and a relatively simple one has been adopted here in which the free-surface boundary conditions (2.6) and (2.7) are expressed in the form

$$\eta_{t+\Delta t} = \eta_t + \tfrac{1}{2}\Delta t\left[3\left\{\frac{1}{n_z}\frac{\partial\phi}{\partial n}\right\}_t - \left\{\frac{1}{n_z}\frac{\partial\phi}{\partial n}\right\}_{t-\Delta t}\right], \tag{2.16}$$

$$\phi_{t+\Delta t} = \phi_t - \tfrac{1}{2}\Delta t[3\{g\eta + \tfrac{1}{2}(\nabla\phi)^2\}_t - \{g\eta + \tfrac{1}{2}(\nabla\phi)^2\}_{t-\Delta t}]. \tag{2.17}$$

The subscripts denote the times at which the corresponding quantities are considered, and each quantity is located on the surface S_f at the corresponding subscripted instant. (One advantage of the formula used above is that the solution's variation with time does not exhibit noticeable oscillatory behaviour. More accurate formulae in Δt may readily be adopted if required.) In applying (2.16) and (2.17), the right-hand sides contain quantities at times t and $t-\Delta t$, which are known from previous iterations, so that the boundary condition is established in the form

$$\phi_{t+\Delta t} = f(t, t-\Delta t) \quad \text{on } S_{f(t+\Delta t)}, \tag{2.18}$$

where $f(\,)$ is a known quantity.

The boundary condition on the immersed body surface is given from (2.5) and (2.8) as

$$\frac{\partial\phi}{\partial n} = \sum_{k=1}^{6} n_k u_k. \tag{2.19}$$

The six values of u_k needed in (2.19) may themselves be determined from the six equations of motion. These may be written (Landweber 1961) as

$$F_k = m_k\dot{u}_k + f_k \quad (k = 1, \ldots, 6), \tag{2.20}$$

with

$$\left.\begin{aligned} f_1 &= m_1(u_5u_3 - u_6u_2),\\ f_2 &= m_2(u_6u_1 - u_4u_3),\\ f_3 &= m_3(u_4u_2 - u_5u_1),\\ f_4 &= -(m_5 - m_6)u_5u_6,\\ f_5 &= -(m_6 - m_4)u_6u_4,\\ f_6 &= -(m_4 - m_5)u_4u_5. \end{aligned}\right\} \tag{2.21}$$

Here F_1, F_2, F_3 denote the components in the x', y', z' directions of the force acting on the body; F_4, F_5, F_6 denote the components about the x', y', z' directions of the moment acting about G; $m_1 = m_2 = m_3$ is the mass of the body; and m_4, m_5 and m_6 are the moments of inertia of the body about the x', y' and z' axes respectively.

The force components F_k are due to the pressure distribution over the body. (In certain applications they may also include mooring forces, or be taken to account empirically for the effects of viscous damping.) Since the motion nonlinearities have been retained, the hydrostatic force components are not separated into linear stiffness terms in the usual way, but rather the pressure used to calculate F_k is taken to include the hydrostatic term. Thus the pressure p over the body is given by the unsteady Bernoulli equation

$$p = -\rho[gz + \dot{\phi} + \tfrac{1}{2}(\nabla\phi)^2], \tag{2.22}$$

where ρ is the fluid density. The force components F_k can be expressed by appropriate integrations of the pressure:

$$F_k = \int_{S_b} p n_k \, dS. \tag{2.23}$$

From the above relations the force components and consequently the velocity components u_k may be found, and thus the body-surface boundary condition specifying $\partial\phi/\partial n$ is established.

The integral equation (2.15) over the surface $S_b + S_f$, in which G is given by (2.11), together with the boundary conditions given by (2.18) and (2.19), may now be solved numerically to obtain the distributions of ϕ and $\partial\phi/\partial n$ over $S_b + S_f$ at time $t + \Delta t$. Time can then be advanced by one step so that the free-surface boundary conditions and the equations of motion can be used to establish (2.18) and (2.19) at the new time. The problem can then be solved at the new time, and in this way the calculations can be advanced over a sufficient duration to describe the evolution of the flow and the body motions with time. This completes an outline of the theoretical basis of the method used, and the numerical procedures based on it are now summarized.

3. Numerical procedure

The surfaces S_b, S_c and S_f are discretized into finite numbers of area elements or facets, as indicated in figure 3. Equation (2.15) and the boundary conditions (2.18) and (2.19) are then made to apply at the corresponding facet centres of S_b and S_f. Thus (2.15) may be rewritten without approximation as

$$\begin{aligned}\phi(\mathbf{x}_i) = {} & \frac{1}{2\pi}\sum_{j=1}^{N}\left\{\int_{\Delta S_j} G(\mathbf{x}_i, \boldsymbol{\xi})\frac{\partial\phi}{\partial n}(\boldsymbol{\xi})\,dS - \int_{\Delta S_j}\phi(\boldsymbol{\xi})\frac{\partial G}{\partial n}(\mathbf{x}_i, \boldsymbol{\xi})\,dS\right\} \\ & + \frac{1}{2\pi}\sum_{j=N+1}^{N'}\left\{\int_{\Delta S_j} G(\mathbf{x}_i, \boldsymbol{\xi})\frac{\partial\phi^{(w)}}{\partial n}(\boldsymbol{\xi})\,dS\right. \\ & \left. - \int_{\Delta S_j}\phi^{(w)}(\boldsymbol{\xi})\frac{\partial G}{\partial n}(\mathbf{x}_i, \boldsymbol{\xi})\,dS\right\} \quad (i = 1, 2, \ldots N),\end{aligned} \tag{3.1}$$

where $\mathbf{x}_i$ is the point $\mathbf{x}$ at the centre of the ith facet, and ΔS_j is the area of the jth facet. N is the number of facets over $S_b + S_f$ (made up of N_b facets over S_b and N_f facets over

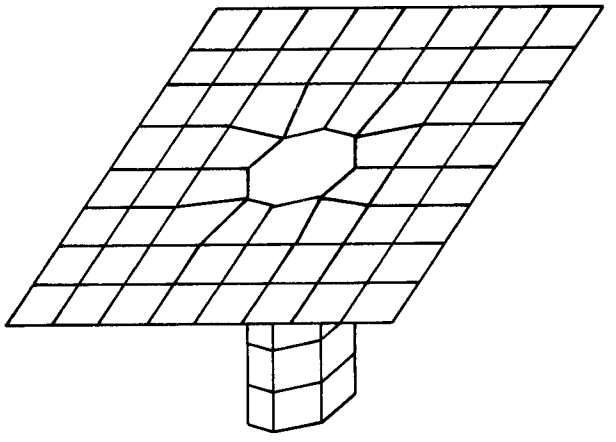

FIGURE 3. Sketch of surfaces discretized into facets (shown with $\eta = 0$).

S_f), N' is the total number of facets and it is understood that the surfaces are treated in the order S_b, S_f, S_c as the index j increases from 1 to N'.

It is possible in principle to develop different-order approximations to the solution in terms of a parameter $\epsilon = \Delta s/L$, where Δs is a characteristic facet length and L is the incident wavelength (Isaacson 1981*a*). To a first such approximation, the integrands in (3.1) are taken as constant over ΔS_j (except for singular terms when $i = j$), and (3.1) may then be written as a set of N linear equations for the $2N$ quantities $\phi_j = \phi(\mathbf{x}_j)$ and $(\partial\phi/\partial n)_j = \partial\phi/\partial n(\mathbf{x}_j)$ over $S_b + S_f$. Thus

$$\sum_{j=1}^{N}\left[a_{ij}\,\phi_j + b_{ij}\left(\frac{\partial\phi}{\partial n}\right)_j\right] = c_i \quad (i = 1, 2, \ldots N), \tag{3.2}$$

where the left-hand side of (3.1) is absorbed into the coefficients a_{ii}. The coefficients c_i are given as

$$c_i = \sum_{j=N+1}^{N'} \frac{\Delta S_j}{2\pi}\left[G_{ij}\left(\frac{\partial\phi^{(w)}}{\partial n}\right)_j - \left(\frac{\partial G}{\partial n}\right)_{ij}\phi_j^{(w)}\right], \tag{3.3}$$

where G_{ij} denotes $G(\mathbf{x}_i, \boldsymbol{\xi}_j)$ and so on. G may be obtained directly in terms of $\mathbf{x}$ and $\boldsymbol{\xi}$ as indicated in (2.11). $\partial G/\partial n$ may be expressed in terms of $\mathbf{x}$, $\boldsymbol{\xi}$ and $\mathbf{n}$ (at $\boldsymbol{\xi}$) as

$$\begin{aligned}\frac{\partial G}{\partial n} &= \frac{\partial(1/r)}{\partial r}\cos\gamma + \frac{\partial(1/r')}{\partial r'}\cos\gamma' \\ &= -\frac{\cos\gamma}{r^2} - \frac{\cos\gamma'}{r'^2}.\end{aligned} \tag{3.4}$$

Here γ and γ' are respectively the angles between $\mathbf{n}$ and $\mathbf{r} = \boldsymbol{\xi} - \mathbf{x}$ and between $\mathbf{n}' = n_x\mathbf{i} + n_y\mathbf{j} - n_z\mathbf{k}$ and $\mathbf{r}' = \boldsymbol{\xi}' - \mathbf{x}$ so that

$$\left.\begin{aligned}\cos\gamma &= \frac{\mathbf{n}\,.\,(\boldsymbol{\xi} - \mathbf{x})}{r}, \\ \cos\gamma' &= \frac{\mathbf{n}'\,.\,(\boldsymbol{\xi}' - \mathbf{x})}{r'}.\end{aligned}\right\} \tag{3.5}$$

When $i \neq j$ the coefficients a_{ij} and b_{ij} are given as

$$a_{ij} = \frac{\Delta S_j}{2\pi}\left(\frac{\partial G}{\partial n}\right)_{ij}, \quad b_{ij} = -\frac{\Delta S_j}{2\pi} G_{ij}. \tag{3.6), (3.7}$$

When $i = j$ the integrands in (3.1) are singular, and the corresponding integrals with ϕ and $\partial\phi/\partial n$ taken as constants may be found analytically for any given facet shape in exactly the same way as is performed in linear diffraction problems. If the non-singular components $1/r'$ and $\partial(1/r')/\partial n$ are taken as constant over each facet as above, then we obtain

$$a_{ii} = 1 - \frac{\Delta S_i (n_z)_i}{8\pi(z_i + d)^2}, \tag{3.8}$$

$$b_{ii} = -\frac{(\Delta S_i)^{\frac{1}{2}}}{2\pi} I - \frac{\Delta S_i}{4\pi(z_i + d)}, \tag{3.9}$$

in which

$$I = \frac{1}{(\Delta S_i)^{\frac{1}{2}}} \int_{\Delta S_i} \frac{1}{r} dS. \tag{3.10}$$

In (3.8) the first term on the right corresponds to the left-hand side of (3.1) and the second term to that involving $\partial(1/r')/\partial n$. The integral I depends only on a particular facet shape as already indicated and may readily be evaluated.

With the coefficients a_{ij}, b_{ij} and c_i now known, (3.2) provides N equations for the N values each of ϕ_j and $(\partial\phi/\partial n)_j$ over $S_b + S_f$. The boundary conditions on the free surface and body are required to specify the location of S_f and to provide the remaining N relations that are needed.

The free-surface boundary conditions are applied at the N_f facet centres on the free surface, and so provide N_f values of ϕ_j. In applying these at any facet centre, an interpolation using the values of η and ϕ at neighbouring facet centres is needed to evaluate some terms on the right-hand sides of (2.16) and (2.17).

The body-surface condition expresses the N_b values of $(\partial\phi/\partial n)_j$ in terms of u_k (at the advanced time $t + \Delta t$). Using the equations of motion, these components may themselves be expressed in terms of ϕ_j at the advanced time $t + \Delta t$, together with the available solution at times t and $t - \Delta t$, as indicated in the following. To a consistent approximation in ϵ, the pressure acting over any one facet may be taken as uniform so that the normal force ΔF_j on the jth facet is simply

$$\Delta F_j = -\rho \Delta S_j [gz + \dot{\phi} + \tfrac{1}{2}(\nabla\phi)^2]_j. \tag{3.11}$$

All such values of ΔF_j may be summed appropriately to obtain the total force components F_k:

$$F_k = \sum_{j=1}^{N_b} (n_k)_j \Delta F_j, \tag{3.12}$$

where $(n_k)_j$ is the value of n_k at the jth facet centre. Substituting (3.11) and (3.12) into the equations of motion (2.20), we have

$$m_k \dot{u}_k = -\rho \sum_{j=1}^{N_b} (n_k)_j \Delta S_j [gz + \dot{\phi} + \tfrac{1}{2}(\nabla\phi)^2]_j - f_k \quad (k = 1, \ldots, 6). \tag{3.13}$$

The components $(u_k)_{t+\Delta t}$ at the advanced time $t+\Delta t$ can be obtained from this equation by a suitable time-differencing procedure. However, the numerical differentiation needed to determine $\dot{\phi}_j$ on the right-hand side may lead to unstable behaviour, and may be circumvented by rewriting (3.13) as

$$m_k \dot{u}_k + \rho \sum_{j=1}^{N_b} \frac{d}{dt}[(n_k)_j \Delta S_j \phi_j]$$
$$= -\rho \sum_{j=1}^{N_b} \left\{(n_k)_j \Delta S_j [gz + \tfrac{1}{2}(\nabla\phi)^2]_j - \phi_j \frac{d}{dt}[(n_k)_j \Delta S_j]\right\} - f_k \quad (k = 1, \ldots, 6). \tag{3.14}$$

The advantage of using this form is that the left-hand side can be integrated directly with respect to time, and the term involving $d[(n_k)_j \Delta S_j]/dt$ is absent in the linear case and should generally be small compared to that based on retaining $\dot{\phi}$ itself on the right-hand side. The same time-differencing equation used previously now gives

$$\left[m_k u_k + \rho \sum_{j=1}^{N_b} (n_k)_j \Delta S_j \phi_j\right]_{t+\Delta t} = H_k \quad (k = 1, \ldots, 6), \tag{3.15}$$

where

$$H_k = \left\{m_k u_k + \rho \sum_{j=1}^{N_b} (n_k)_j \Delta S_j \phi_j\right\}_t - \tfrac{1}{2}\Delta t\,[3(h_k)_t - (h_k)_{t-\Delta t}], \tag{3.16}$$

$$h_k = \rho \sum_{j=1}^{N_b} \left\{(n_k)_j \Delta S_j [gz + \tfrac{1}{2}(\nabla\phi)^2]_j - \phi_j \frac{d}{dt}[(n_k)_j \Delta S_j]\right\} + f_k$$

We are now in a position to revert to the solution of (3.2). Taking into account (2.19) and (3.15) above, (3.2) together with the boundary conditions on the free surface and the body surface may be expressed in a compact form in terms of unknowns ψ_j which contain all the unknown values of ϕ_j (over S_b) and $(\partial\phi/\partial n)_j$ (over S_f) at the advanced time $t+\Delta t$. Thus

$$\sum_{j=1}^{N} A_{ij}\psi_j = \lambda_i \quad (i = 1, 2, \ldots, N), \tag{3.17}$$

in which

$$\psi_j = \begin{cases} \phi_j & (j = 1, \ldots, N_b), \qquad (3.18a) \\ \left(\dfrac{\partial\phi}{\partial n}\right)_j & (j = N_b + 1, \ldots, N), \qquad (3.18b) \end{cases}$$

$$A_{ij} = \begin{cases} a_{ij} - \displaystyle\sum_{l=1}^{N_b} b_{il} \sum_{k=1}^{6} \frac{\rho}{m_k}(n_k)_l (n_k)_j \Delta S_j & (j = 1, \ldots, N_b), \qquad (3.19a) \\ b_{ij} \quad (j = N_b + 1, \ldots, N), & \qquad (3.19b) \end{cases}$$

$$\lambda_i = c_i - \sum_{j=N_b+1}^{N} a_{ij}\phi_j - \sum_{j=1}^{N_b} b_{ij} \sum_{k=1}^{6} (n_k)_j \frac{H_k}{m_k}. \tag{3.20}$$

The solution to this matrix equation may be readily obtained.

In carrying out this procedure for successive time steps, the various quantities of direct interest can be retrieved as required. In particular the forces on the body may be obtained from (3.11) and (3.12), and the velocity components u_k may be obtained from (3.15). The body motions defined by the co-ordinates ζ_k are also required and can now be obtained by solving first (2.1) and then (2.2).

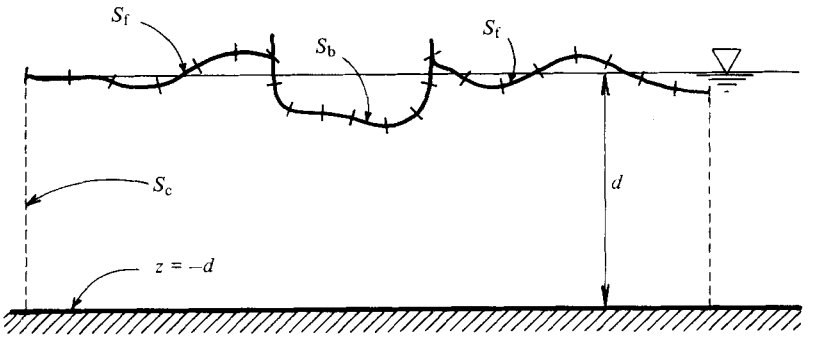

FIGURE 4. Sketch of discretized surfaces for the vertical-plane case.

By modifying (3.13) to (3.20) as needed, it is relatively straightforward to treat related problems in which the body motions may be prescribed as in forced-motion problems, or restricted, for example, to heave oscillations only, to the case of a moored body, or to the special case of a fixed body.

The whole procedure can now be carried out so that the development of the flow, the forces and the motions of the body may be obtained. The procedure is started at a time when the incident wave velocity at the body surface is zero so that the initial conditions are known, with S_f then corresponding to the incident wave profile.

In applying the method, it is noted that the facet locations and orientations must be adjusted at each time step, and this involves co-ordinate transformations between the $Oxyz$ and $Gx'y'z'$ systems. Furthermore, when the free-surface facets undergo a horizontal shift over a time step the form of the boundary conditions used must account for the changes to facet-centre location. For example, the corresponding modification to (2.16) would be based on the approximation

$$\eta_{t+\Delta t}(s_{t+\Delta t}) = \eta_t(s_t) + \tfrac{1}{2}\Delta t[3\dot{\eta}_t(s_t) - \dot{\eta}_{t-\Delta t}(s_{t-\Delta t})] + \tfrac{1}{2}\Delta s\left[3\left(\frac{\partial \eta}{\partial s}\right)_t(s_t) - \left(\frac{\partial \eta}{\partial s}\right)_{t-\Delta t}(s_{t-\Delta t})\right], \tag{3.21}$$

where s denotes the location at which η is taken and itself depends on time. Similar corrections need to be taken into account also in the other relationships involving segment locations at different instants, as in (2.17).

4. Vertical-plane problems

A simplification to the method described here may readily be adopted to treat corresponding two-dimensional problems in the vertical (x, z)-plane. For the fixed-body case, this problem has also been treated by Vinje & Brevig (1981) using a different method. The body now possesses three degrees of freedom: $u_2 = u_4 = u_6 = 0$. In adapting the method used here, the surface-integral equation deriving from Green's theorem (2.10) reduces to a line-integral equation in which the influence of the co-ordinate y is absent, the factor $1/2\pi$ is replaced by $-1/\pi$ (e.g. Kellogg 1929), and also the Green function is now logarithmic:

$$G = \ln r + \ln r'. \tag{4.1}$$

The integral is separated as before into one over S_c, which is known, and one over $S_b + S_f$. The boundary conditions to this integral equation over $S_b + S_f$ are given by

(2.18) and (2.19) as before. The contour S is now divided into a number of short straight segments as sketched in figure 4, and the integral equation together with its boundary conditions are made to apply at the centre of each segment on $S_b + S_f$. This gives rise to a set of linear equations for ϕ_j and $(\partial\phi/\partial n)_j$ as in (3.2). However, in the vertical-plane case now being considered the coefficients c_i, a_{ij} and b_{ij} are different on account of the different integral equation and Green function that are now applicable. These are now given as

$$c_i = -\sum_{j=N+1}^{N'} \frac{\Delta S_j}{\pi}\left[G_{ij}\left(\frac{\partial\phi^{(w)}}{\partial n}\right)_j - \left(\frac{\partial G}{\partial n}\right)_{ij}\phi_j^{(w)}\right], \tag{4.2}$$

$$a_{ij} = -\frac{\Delta S_j}{\pi}\left(\frac{\partial G}{\partial n}\right)_{ij} \quad (i \neq j), \tag{4.3}$$

$$b_{ij} = \frac{\Delta S_j}{\pi} G_{ij} \quad (i \neq j), \tag{4.4}$$

$$a_{ii} = 1 - \frac{\Delta S_i \cos\gamma'}{2\pi(z_i + d)}, \tag{4.5}$$

$$b_{ii} = \frac{\Delta S_i}{\pi}[\ln \Delta S_i + \ln(z_i + d) - 1]. \tag{4.6}$$

$\partial G/\partial n$ is now calculated from the formula

$$\frac{\partial G}{\partial n} = \frac{\cos\gamma}{r} + \frac{\cos\gamma'}{r'}, \tag{4.7}$$

and γ and γ' are given as before by (3.5). The integral analogous to I in (3.10) is now unique and has been evaluated and substituted into (4.6) above.

The set of linear equations corresponding to (3.17)–(3.20) can now be set up and solved in the same way as before. Once the values of ϕ_j and $(\partial\phi/\partial n)_j$ at the facet centres are known, the wave loads and motions can be calculated by the use of (3.11), (3.12) and (3.15). A considerable simplification in setting up the procedure arises in the calculation of n_z and $(\nabla\phi)^2$ by interpolating from η- and ϕ-values at neighbouring segment centres.

5. Discussion

Various aspects of the numerical procedure described here have been considered by Isaacson (1981*a*) in the context of the fixed-body case. These include a suitable discretization of the free surface, and assessments of possible numerical instabilities and of the accuracy and computational efficiency of the method. Brief mention is made here of the stability and accuracy of the method and of the incident wave representation used.

5.1. *Stability and accuracy*

In analogy with other problems that incorporate time-stepping, the usual condition that is necessary for stability (which may, however, be insufficient) requires that $\Delta t/T$ is sufficiently small compared with $\epsilon(= \Delta s/L)$, where T and L are the incident wave period and wavelength respectively. However, even with reasonably small

values of Δt stability may be difficult to achieve for very steep waves, although it may then be possible to suppress any unstable behaviour by a smoothing procedure (see e.g. Longuet-Higgins & Cokelet 1976).

Quite apart from the question of stability, the accuracy of the solution must also be assessed. Errors may be associated with the time increment Δt or spatial increment Δs. However, errors directly associated with a wave-height perturbation parameter, such as in solutions based on Stokes or cnoidal wave expansions, are avoided in the present case except through the incident wave representation adopted.

Truncation errors involving the interval Δt may be reduced in a reasonably straightforward way by employing a higher-order time-stepping scheme (see e.g. Longuet-Higgins & Cokelet 1976). The approximation in which ϕ and $\partial\phi/\partial n$ are taken to be constant over each facet, and their values at neighbouring facet centres are used to calculate spatial gradients, represents a first approximation in the parameter $\epsilon = \Delta s/L$ (Isaacson 1981*a*), and is equivalent to one generally made in linear diffraction programs.

5.2. *Incident wave representation*

One difficulty in applying the present method concerns a suitable representation of the incident waves such that there is initially no flow immediately adjacent to the body. The special case of a solitary wave fulfils this requirement, but is of restricted application. More generally, an incident-wave flow with still water ahead of the waves is unsteady, and should be treated formally by a time-stepping procedure, such as that indicated by Fenton & Rienecker (1980). However, the difficulty is overcome here by a heuristic approach in which the permanent-wave profile is modified to provide a smooth transition from still water ahead of the wavetrain to the fully established wave flow. This procedure is not rigorous, but can be justified for shallow water and intermediate depth conditions by analogy with the hyperbolic-wave approximation to cnoidal-wave theory. In this approximation, the flow associated with any one wave of a periodic train is represented by a non-periodic decaying function, so that the flow of the wave can be taken effectively to evolve from still water. This is equivalent to the matched solitary-wave approximation utilized by Stiassnie & Peregrine (1980). It is noted that the initial condition employed here differs from the one that has been used by other authors to examine breaking-wave behaviour, in which the flow is taken to start from a large-amplitude *sinusoidal* motion (see e.g. Longuet-Higgins & Cokelet 1976; Srokosz 1981).

6. Results

A computer program based on the method described here has been used to provide preliminary comparisons with available solutions for the cases of both linear- and solitary-wave diffraction around a fixed surface-piercing vertical circular cylinder (Isaacson 1981*a*). A comparison with the solitary-wave solution is particularly relevant here because it provides an independent means of testing the numerical method under nonlinear conditions (even though a small-wave-height assumption is used, with terms of order $(H/d)^2$ omitted), and also it directly satisfies the initial condition of no flow adjacent to the body. A first approximation for the solitary wave case has been given in closed form by Isaacson (1981*a*, 1982*b*) and is essentially an extension to the cnoidal-wave case given previously (Isaacson 1977).

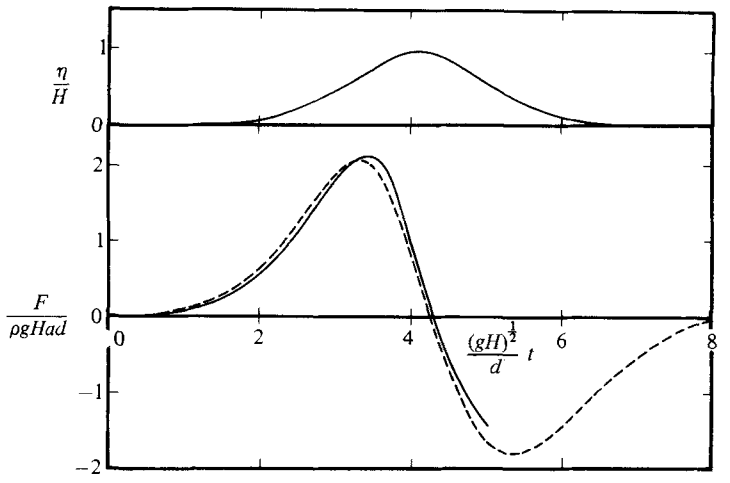

FIGURE 5. Wave-force variation for a solitary wave propagating past a fixed vertical circular cylinder with $d/a = 0{\cdot}5$ and $H/d = 0{\cdot}1$. – – –, closed-form solution (Isaacson 1981*a*, 1982*b*).

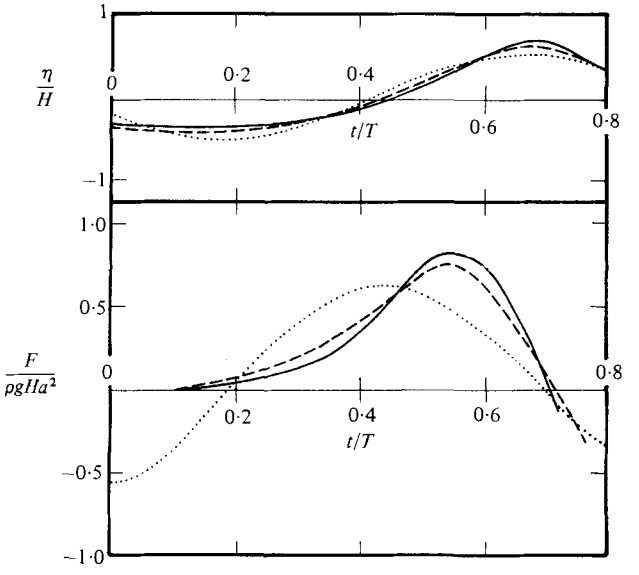

FIGURE 6. Horizontal wave-force variation for a fixed truncated circular cylinder at the free surface, with $d/a = 1{\cdot}5$, $h/a = 0{\cdot}5$ and $d/gT^2 = 0{\cdot}0186$. – – –, $H/d = \frac{1}{4}$; ——, $H/d = \frac{1}{3}$; . . ., linear diffraction solution.

A comparison is presented here for the particular conditions $d/a = 0{\cdot}5$ and $H/d = 0{\cdot}1$, where a is the cylinder radius and H the wave height. The computation was carried out using 100 time steps covering a duration corresponding to $(gH)^{\frac{1}{2}}t/d = 5{\cdot}0$. This spans the important force variation for the case treated. The cylinder surface was discretized into 48 facets, and the free surface into 180 facets. Figure 5 shows the horizontal force variation with time calculated by the present method, together with that obtained from the closed-form solution indicated by the broken line. Also included for reference is the incident wave elevation at $x = 0$. The force variations predicted by both methods are seen to agree reasonably well. For the case treated,

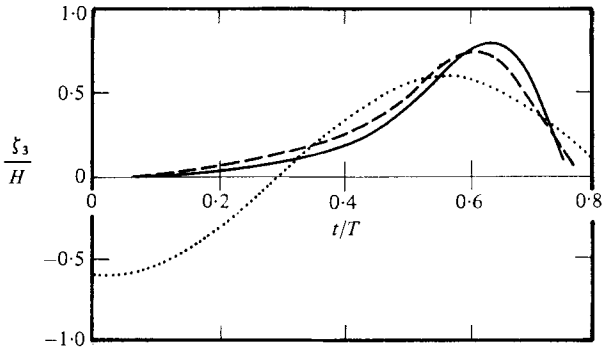

FIGURE 7. Heave variation for conditions corresponding to those of figure 6, except that the cylinder is freely floating with $z_G/h = -\frac{1}{4}$ initially and $m_4/\rho a^5 = 0{\cdot}47$.

the maximum force predicted is within 5% of that predicted by the closed-form solution.

As a more general illustration of the method, results are presented for a truncated vertical circular cylinder at the free surface (a circular dock). The cases treated correspond to $d/a = 1{\cdot}5a$, $h/a = 0{\cdot}5a$, $d/gT^2 = 0{\cdot}0186$ and $H/d = \frac{1}{4}$ and $\frac{1}{3}$ in turn, where h is the cylinder draft and T is the wave period. These waves are reasonably shallow with $d/L \simeq 0{\cdot}15$.

The results are shown in figures 6 and 7. The incident-wave profile for both waves, together with the corresponding linear-wave prediction for permanent waves, are included in figure 6 for reference purposes. The horizontal force for the two cases, together with the corresponding predictions of linear wave theory (Garrett 1971) are shown as functions of time in figure 6 for the case when the cylinder is held fixed. The present method predicts the maximum horizontal force coefficients to be $F/\rho gHa^2 = 0{\cdot}75$ and $0{\cdot}83$ for the two cases, and to occur somewhat closer to an incident wave crest than predicted by linear theory. These maximum force coefficients are respectively about 20 and 32% greater than the linear-theory predictions, and on the basis of inertia-force considerations, are not unexpected.

When the cylinder is freely floating with its centre of mass z_G initially at $z = -\frac{1}{4}h$ and with a radius of gyration in pitch of $0{\cdot}55a$ (i.e. $m_4/\rho a^5 = 0{\cdot}47$), the heave motions as a function of time are shown in figure 7. (The linear theory predictions for this floating-cylinder case are based on an axisymmetric source distribution program (Isaacson 1982*a*).) Once more the apparent differences from linear-theory predictions may be anticipated on the basis of inertia-force behaviour.

7. Conclusions

A numerical method has been developed for the computation of nonlinear ocean-wave interactions with large fixed or floating structures of arbitrary shape. The method involves the application of Green's theorem, and a time-stepping procedure is used to obtain the development of the flow. The method may be simplified to treat corresponding two-dimensional problems in the vertical plane.

Comparisons have been made with known results for the particular cases of small-amplitude sinusoidal- and solitary-wave diffraction around a fixed vertical circular

cylinder, and these are quite favourable. Results are presented for the more general case of a truncated vertical circular cylinder which may be fixed or freely floating, and these exhibit significant differences from linear-theory predictions.

REFERENCES

FENTON, J. D. & RIENECKER, M. M. 1980 Accurate numerical solutions for nonlinear waves. In *Proc. 17th Coastal Engng Conf., Sydney*, pp. 50–69. A.S.C.E.

GARRETT, C. J. R. 1971 Wave forces on a circular dock. *J. Fluid Mech.* **46**, 129–139.

ISAACSON, M. DE ST Q. 1977 Shallow wave diffraction around large cylinder. *J. Waterway, Port, Coastal & Ocean Div. A.S.C.E.* **103** (WW1), 69–82.

ISAACSON, M. DE ST Q. 1981*a* Nonlinear wave forces on large offshore structures. *Coastal/Ocean Engng Rep., Dept Civil Engng, Univ. British Columbia.*

ISAACSON, M. DE ST Q. 1981*b* Steep wave effects on large offshore structures. *Proc. Offshore Tech. Conf., Houston, Paper* no. OTC 3955.

ISAACSON, M. DE ST Q. 1982*a* Fixed and floating axisymmetric bodies in waves. *J. Waterway, Port, Coastal & Ocean Div. A.S.C.E.* **108** (WW2) (in press).

ISAACSON, M. DE ST Q. 1982*b* Solitary wave diffraction around large cylinder. *J. Waterway, Port, Coastal & Ocean Div. A.S.C.E.* (in press).

KELLOGG, O. D. 1929 *Foundations of Potential Theory.* Springer.

LANDWEBER, L. 1981 Motion of immersed and floating bodies. In *Handbook of Fluid Dynamics* (ed. V. L. Streeter), pp. 13-1–13-50. McGraw-Hill.

LONGUET-HIGGINS, M. S. & COKELET, E. D. 1976 The deformation of steep surface waves on water. I. A numerical method of computation. *Proc. R. Soc. Lond.* A **350**, 1–25.

MORSE, P. M. & FESHBACH, H. 1953 *Methods of Theoretical Physics.* McGraw-Hill.

SARPKAYA, T. & ISAACSON, M. 1981 *Mechanics of Wave Forces on Offshore Structures.* Van Nostrand Reinhold.

SROKOSZ, M. A. 1981 Breaking effects in standing and reflected waves. *Preprints, Int. Symp. on Hydrodynamics in Ocean Engng, Trondheim, Norway*, pp. 183–202. Norwegian Hydrodyn. Labs.

STIASSNIE, M. & PEREGRINE, D. H. 1980 Shoaling of finite-amplitude surface waves on water of slowly-varying depth. *J. Fluid Mech.* **97**, 783–805.

VINJE, T. & BREVIG, P. 1981 Numerical calculations of forces from breaking waves. *Preprints, Int. Symp. on Hydrodynamics in Ocean Engng, Trondheim, Norway*, pp. 547–566.